ERC Advanced Grant 2023
Research proposal [Part B2]

Automated Model Discovery for Soft Matter Systems

DISCOVER

Ellen Kuhl
Friedrich-Alexander-Universität Erlangen-Nürnberg (FAU)

Proposal Duration 60 Months

Section a. State-of-the-art and objectives

I. STATE-OF-THE-ART.

Soft materials play an integral role in many aspects of modern life including biomedicine, energy storage, and consumer goods, and their accurate modeling is critical to understand their unique properties and functions. The objective of this project is to integrate theory, experiment, and computation to automatically discover the models, parameters, and experiments that best explain a wide variety of natural and man-made soft matter systems as illustrated in Figure 1.

Figure 1. This project will integrate theory, experiment, and computation to automatically discover the models, parameters, and experiments that best explain a wide variety of natural and man-made soft matter systems including the heart, arteries, muscle, lung, liver, skin, brain, hydrogels, silicone, artificial meat, foams, and rubber. My main deliverable is a open source scientific discovery platform that will include our new constitutive neural networks, experimental data, benchmarks, models, and parameters, fully documented and freely accessible on GitHub @LivingMatterLab.

Soft materials are complex to understand and challenging to model. For decades, chemical, physical, and material scientists alike have been modeling the hyperelastic response of soft matter under finite deformations[12,85,89,131]. They have proposed numerous competing constitutive models to best characterize the behavior of natural and man-made soft materials and calibrated their model parameters using uniaxial tension, compression, shear, and biaxial tests[23,40,48,49]. With this proposal, I challenge the conventional wisdom and propose a radically different approach towards constitutive modeling: I abandon the common strategy to *first* select a constitutive model and *then* tune its parameters by fitting the model to data[50,57,63,107,120]. Instead, I propose to *simultaneously* and *fully autonomously* discover both the constitutive model and the material parameters that best explain the experimental data. While constitutive models for stiff materials are well-studied and well-understood, soft materials typically undergo finite deformations[129]; they are highly nonlinear, often incompressible[130], anisotropic[119], tension-compression asymmetric[21], and generally challenging to model[138]. Two classes of models have emerged to simulate soft materials, models in terms of the principal invariants[50], $I_1 = \text{tr}(\mathbf{C})$, $I_2 = \frac{1}{2}[\,\text{tr}^2(\mathbf{C}) - \text{tr}(\mathbf{C}^2)]$, $I_3 = \det(\mathbf{C})$, with a free energy function, $\psi(I_1, I_2, I_3)$, and models in terms of the principal stretches[89,133], $\lambda_1, \lambda_2, \lambda_3$, with a free energy function, $\psi(\lambda_1, \lambda_2, \lambda_3)$. In

finite deformations, $\mathbf{F} = d\mathbf{x} / d\mathbf{X}$ is the deformation gradient, $\mathbf{C} = \mathbf{F}^t \cdot \mathbf{F}$ is the right Cauchy Green deformation tensor, and the squared stretches λ_i^2 are its eigenvalues, $\mathbf{C} = \Sigma_i \lambda_i^2 \mathbf{N}_i \otimes \mathbf{N}_i$. The choice of the appropriate invariant- or principal-stretch-based model depends largely on user experience and personal preference. In the age of machine learning, this raises the question: Can we leverage the power of neural networks to systematically learn the best constitutive models for soft matter systems?

Classical neural networks interpolate data well, but ignore the underlying physics. In the most general form, constitutive equations in solid mechanics are tensor-valued tensor functions that define the relation between a stress, for example the Piola stress, $\boldsymbol{P} = \lim_{d\mathbf{A}\to 0} (d\mathbf{f} / d\mathbf{A})$, as the force $d\mathbf{f}$ per undeformed area $d\mathbf{A}$, and a deformation measure, for example the deformation gradient $\boldsymbol{F}$[50,129]. Conceptually, we could use any neural network as a function approximator[81] to learn the relation between $\boldsymbol{P}$ and $\boldsymbol{F}$, and many approaches in the literature, including the one in Figure 2, actually do exactly that[3,41,52,79]. Interestingly, the first neural network that learned a stress-strain model from data was proposed for concrete more than three decades ago[41]. In the early days[53], neural networks served merely as regression operators and were commonly viewed as a black box. This lack of transparency is probably the main reason why these early approaches never really generated momentum in our mechanics community. Now, more than 20 years later, neural networks have advanced as a promising technology to support constitutive modeling. They hold a tremendous potential to interpolate big data, especially when we have no prior information about the data[5]. However, they generally perform poorly on small data, they are at risk of overfitting[62], and fail to extrapolate or predict scenarios beyond their training regime[93]. More importantly, classical off-the-shelf neural networks entirely ignore our prior domain knowledge and the functions $\boldsymbol{P}(\boldsymbol{F})$ that they learn often violate standard arguments of thermodynamics and widely-accepted physical constraints[42]. This motivates the question whether and how we can build our prior domain knowledge in soft matter physics into a neural network.

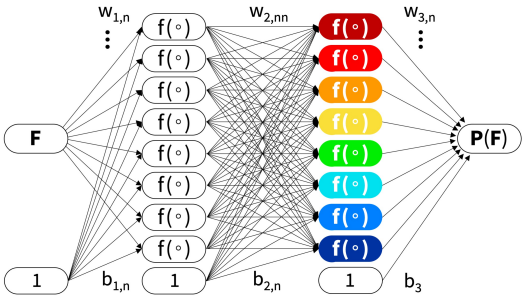

Figure 2. Classical neural network with two fully connected hidden layers and eight nodes per layer to approximate the nine components of the Piola stress $\mathbf{P}(\mathbf{F})$ as functions of the nine components of the deformation gradient $\mathbf{F}$ using 80 weights, 17 biases, and a total of 97 parameters[74].

Physics informed neural networks integrate physics into the loss function. Two successful but fundamentally different strategies have emerged to integrate physical knowledge into network modeling, physics informed neural networks that add physics equations as additional terms to the loss function[60], see Figure 3, and constitutive artificial neural networks that explicitly modify the network input, output, and architecture to hardwire physical constraints into the network design[71], see Figure 6. The former are more general and typically work well for ordinary[11,72] or partial[5,97,101] differential equations, while the latter are specifically tailored towards constitutive equations[73,74]. In fact, one such neural network, with strain invariants as input, free energy functions as output, and a single hidden layer with logistic activation functions in between, has been proposed for rubber materials almost two decades ago[118] and recently regained attention in the constitutive modeling community[71,146]. While these constitutive neural networks generally provide an excellent fit to experimental data, how exactly they can best integrate thermodynamic constraints remains a question of ongoing debate[80].

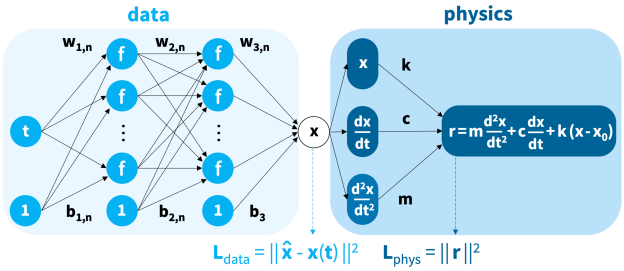

Figure 3. Physics-informed neural networks minimize a loss function $L \to \min$ that consists of a data loss L_{data}, the error between data and model $|| \mathbf{x} - \mathbf{x}(\mathbf{t}) ||$, and a physics loss L_{phys}, the physics residual $|| \mathbf{r} ||$, to learn the network parameters, $\boldsymbol{\theta} = \{ \mathbf{w}, \mathbf{b} \}$ and the physics parameters $\boldsymbol{\vartheta} = \{ k, c, m \}$ [72].

Constitutive neural networks hardwire physical constraints into the network design. Constitutive artificial neural networks a priori build the first and second law of thermodynamics into the network architecture[79] and select specific activation functions to ensure compliance with thermodynamic constraints[74]. Recent studies suggest that this approach can successfully reproduce the constitutive behavior of rubber-like materials[42]. Alternative approaches use a regular neural network and ensure

thermodynamic consistency a posteriori via a pseudo-potential correction in a post processing step[58]. To demonstrate the versatility of these different approaches, several recent studies have successfully embedded constitutive neural networks in a finite element analysis, for example, to model plane rubber sheets[71], sheets with holes[127], or entire tires[118], the numerical homogenization of discrete lattice structures[80], microstructures with inclusions[4], evolving microstructures[144], the deployment of parachutes[7], or surgical procedures[124]. Regardless of all these success stories, one major limitation remains: the lack of an intuitive interpretation of the network model and its parameters[62].

Constitutive neural networks can be reverse-engineered from constitutive building blocks. To understand the art of modeling, it is insightful to perform a systematic comparison of classical popular constitutive models[77,121]. Strikingly, the most widely used constitutive models are made up of structurally and functionally similar building blocks[34,37,46]. They are either functions of the set of invariants[50], I_1, I_2, I_3, or of the set of principal stretches[89], λ_1, λ_2, λ_3, or more precisely, their equivalents in the undeformed reference configuration, $[I_1\text{-}3]$, $[I_2\text{-}3]$, $[I_3\text{-}1]$, or $[\lambda_1\text{-}1]$, $[\lambda_2\text{-}1]$, $[\lambda_3\text{-}1]$. These kinematic descriptors are then raised to linear, quadratic, or higher order powers, $(\circ)^1$, $(\circ)^2$,…, $(\circ)^n$, as in the neo Hooke[132], Blatz Ko[12], and Mooney Rivlin[85,102] models, and possibly further integrated into exponential or logarithmic functions, $[\exp(\circ)\text{-}1]$ or $[\ln(1\text{-}(\circ))]$, as in the Demiray[22,23], Gent[40], and Holzapfel[49] models. Coefficients of these models, or combinations of them, take the natural interpretation of the shear and bulk moduli or Lamé constants. A natural question to ask is whether and how we can reverse engineer *our own* family of constitutive neural networks[13] with activation functions that feature these popular constitutive building blocks and network weights that translate into well-known engineering parameters.

II. PRELIMINARY RESULTS.

My research group has successfully tested[17,18,95,139,141,142], modeled[19,20,43,47,64,84,122,135], and simulated soft materials[24,25,30,31,33,65,112,113,145] and fit our models to data[18,19,21,114,115]. However, it is becoming increasingly clear that this approach provides only limited insight into the complex behavior of soft materials. To gain a more holistic understanding, we will now establish an open source discovery platform that autonomously discovers the best model, parameters, and experiments for a wide variety of soft matter systems.

Triaxial soft matter testing reveals different stiffnesses in tension, compression, and shear. Numerous well-documented experiments exist in the literature to calibrate the constitutive models for soft materials[27,103,132]. However, most often, these tests are only performed for a single loading mode and fail to predict the behavior of soft matter systems under arbitrary loading conditions[21]. To fully characterize the three-dimensional response of human brain gray and white matter tissue, we conducted a sequence of multiple loading modes, tension, compression, and shear, all on the same specimens[18], see Figure 4. In a close collaboration with Professor Gerhard Holzapfel at the Institute of Biomechanics of TU Graz, we performed a total of n = 276 tests on 5×5×5 mm^3 sized cubical samples from the cortex, basal ganglia, corona radiata, and corpus callosum of ten human brains, with a three-axes force-sensor (K3D40, ME-Measuring Equipment, Henningsdorf, Germany), with motor control and data acquisition using the software testXpert II (Zwick/Roell GmbH & Co. KG, Ulm, Germany). We found that human brain tissue is nonlinear, with a pronounced tension-compression asymmetry[21]. Across all four brain regions, the shear modulus was largest in compression with μ = 0.99 - 2.80 kPa, followed by shear with μ = 0.53 – 1.95 kPa, and tension with μ = 0.29 - 1.22 kPa[18]. Our results suggest that constitutive models for soft materials must be tension-compression asymmetric, and that the parameters identified for a single loading mode likely under- or overestimate the stiffnesses under arbitrary loading conditions.

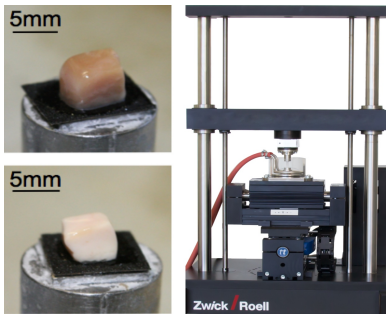

Figure 4. Our triaxial testing of soft materials in tension, compression, and shear revealed a highly non-linear and asymmetric material behavior[18].

Parameter values are highly sensitive to the underlying model. The current gold standard in constitutive modeling is to first select a constitutive model and then fit its parameters to data. We have successfully used our tension, compression, and shear data from Figure 5 to fit the parameters of popular constitutive models[18], including the neo Hooke model[138] with $\psi = \frac{1}{2}\mu\,[\,I_1 - 3\,]$, the Mooney Rivlin model[85,102] with $\psi = \frac{1}{2}\mu_1\,[\,I_1 - 3\,] + \frac{1}{2}\mu_2\,[\,I_2 - 3\,]$, the Demiray model[23] with $\psi = \frac{1}{2}\mu\,[\,\exp(b\,[\,I_1 - 3\,])-1]$, the

Gent model[40] with $\psi = -\frac{1}{2}\,\mu\,\ln(1-(\beta\,[\,I_1 - 3\,]))/\beta$, and the one-term Ogden model[89] with $\psi = 2/\mu\,\Sigma_i\,[\,\lambda_i^{\alpha} - 1\,]/\alpha^2$. We found that, across all five models, the shear moduli in the softest region, the corpus callosum, varied between $\mu = 0.35$ kPa and $\mu = 0.65$ kPa, and in the stiffest region, the cortex, between $\mu = 1.35$ kPa and $\mu = 2.08$ kPa. Strikingly, across all tests and brain regions, the shear stiffnesses predicted by the neo Hooke model were up to 2.3 times larger than those of the Ogden model[18]. This suggest that the shear moduli, and possibly other parameters, are highly sensitive to model selection, and that reporting parameters without reference to the underlying model could under- or overestimate the material behavior.

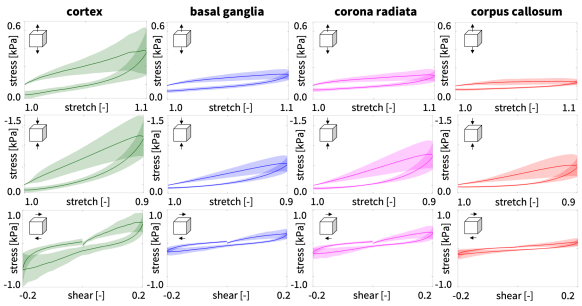

Figure 5. Our triaxial testing of gray and white matter from four brain regions revealed the stiffest response in compression and the softest in tension[21]. Graphs report means and standard deviations of a total of n = 276 tests.

Our constitutive neural networks satisfy common thermodynamic constraints. First, to ensure thermodynamic consistency, instead of approximating the nine components of the Piola stress $\boldsymbol{P}(\boldsymbol{F})$, our constitutive neural networks approximate the scalar-valued free energy function $\psi(\boldsymbol{F})$ and derive the stress $\boldsymbol{P}$ in a post-processing step[71,88,94], $\boldsymbol{P} = \partial\psi/\partial\boldsymbol{F}$. Satisfying thermodynamic consistency directly affects the output of our neural network. Second, to a priori satisfy material objectivity or frame indifference, we require that the arguments of the free energy function are independent of rotations, and are functions of the right Cauchy Green deformation tensor[129], $\boldsymbol{P} = \partial\psi(\boldsymbol{C})/\partial\boldsymbol{F} = 2\boldsymbol{F}\cdot\partial\psi(\boldsymbol{C})/\partial\boldsymbol{C}$. Satisfying material objectivity directly affects the input of our neural network. Third, to include material symmetry, we consider the special case of isotropy, for which the free energy function is a function of the strain invariants[50], $\boldsymbol{P} = \partial\psi(I_1, I_2, I_3)/\partial\boldsymbol{F}$. Considering materials with known symmetry classes directly affects the input of our neural network. Fourth, we consider the special case of perfect incompressibility, $I_3 = J^2 = 1$, for which the free energy function depends only on the first and second invariants I_1 and I_2, corrected by a pressure term[75], $\boldsymbol{P} = \partial\psi(I_1, I_2)/\partial\boldsymbol{F} - p\,\boldsymbol{F}^{-t}$. Perfect incompressibility reduces the input of our neural network. Fifth, we include further physical constraints[6] by assuming that the free energy is non-negative for all deformation states, $\psi(\boldsymbol{F}) \geq 0$; the free energy and the stresses are zero, $\psi(\boldsymbol{F}) = 0$ and $\boldsymbol{P}(\boldsymbol{F}) = \boldsymbol{0}$, in the reference configuration, $\boldsymbol{F} = \boldsymbol{I}$, and the free energy is infinite, $\psi(\boldsymbol{F}) \to \infty$, for infinite compression, $J \to 0$, and infinite expansion, $J \to \infty$. Satisfying these physical constraints directly affects the choice of the activation functions of our neural network. Sixth, to ensure polyconvexity[9], we select a free energy function ψ that is the sum of individual polyconvex subfunctions[46], ψ_1 and ψ_2, such that $\boldsymbol{P} = \partial\psi_1/\partial I_1 \cdot \partial I_1/\partial\boldsymbol{F} + \partial\psi_2/\partial I_2 \cdot \partial I_2/\partial\boldsymbol{F} - p\,\boldsymbol{F}^{-t}$. Satisfying polyconvexity is associated with non-negative network weights and affects the architecture and connectedness of our neural network, as illustrated in Figure 6.

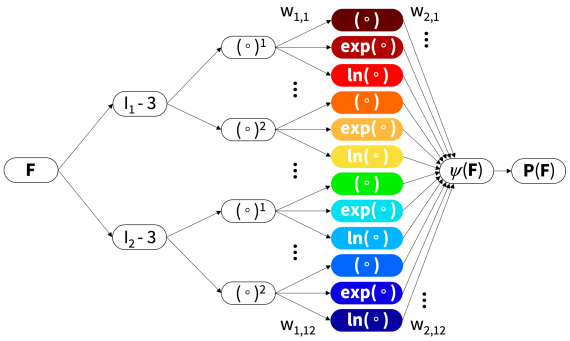

Figure 6. Our constitutive neural network for isotropic incompressible materials approximates the free energy function $\psi(I_1, I_2)$ as a function of the invariants I_1, I_2 of the deformation gradient **F** using 24 weights in total[75].

Our neural network robustly discovers a four-term model for gray matter. When trained with individual tension, compression, and shear data, our network in Figure 6 trains robustly and converges within less than 5,000 epochs with R^2 values of 0.99, 1.00, 1.00 within 2-3 minutes on a standard desktop computer[75]. However, the broad color spectrum in Figure 7 indicates that the network discovers a wide range of terms. Notably, when trained with all data combined, right column, the network robustly discovers a four-term model that only features the second invariant, $\psi(I_2) = \frac{1}{2}\,\mu_2\,[\,I_2 - 3\,]^2 + \frac{1}{2}\,a_2/b_2\,[\exp(b_2$

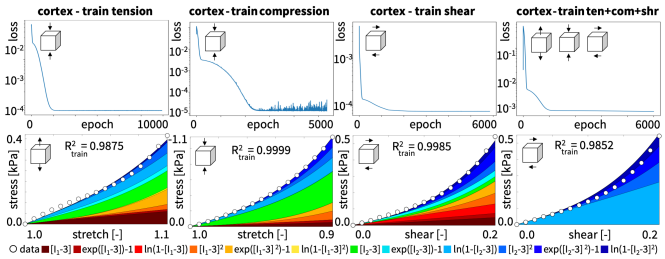

Figure 7. Model and parameter discovery for gray matter. Convergence of loss function, top, and stress response, bottom; dots illustrate experimental data; color code highlights the terms of the discovered model according to Figure 6 [75].

$[I_2\text{-}3]^2$) -1] - ½ α_1/β_1 ln(1-(β_1 [I_2-3])) - ½ α_2/β_2 ln(1-(β_2 [I_2-3] ^{2})), while the weights of the other eight terms consistently train to zero. The non-zero weights naturally translate into physically meaningful parameters with well-defined physical units: four stiffness-like parameters μ_2 = 7.60 kPa, a_2 = 6.23 kPa, α_1 = 1.25 kPa, and α_2 = 4.67 kPa, and three nonlinearity parameters, b_2 = 1.65, β_1 = 0.99, and β_2 = 1.40 [75].

III. OBJECTIVES.

My long-term goal is to democratize constitutive modeling through automated model discovery and make it accessible to a more inclusive and diverse community of students, scientists, and industries to accelerate the design of new functional materials and structures with tailored material properties. The overall objective of this proposal is to establish, train, test, and validate a new family of constitutive neural networks that simultaneously and fully autonomously discover the model, parameters, and experiment that best explain the behavior of a wide variety of soft materials. My project will provide unprecedented new insights into constitutive modeling that are out of reach with traditional theoretical and numerical approaches today. I will achieve these goals by completing three work packages:

WP 1. Establish a new family of constitutive neural networks that reproducibly discover the model, parameters, and experiment that best explain a wide variety of soft matter systems.

WP 2. Quantify the performance of our discovered models on previously unseen data for the heart, arteries, muscle, lung, liver, skin, brain, hydrogels, silicone, artificial meat, foams, and rubber.

WP 3. Quantify the uncertainty of our models, parameters, and experiments by embedding our networks into a Bayesian analysis to discover parameter distributions and credible intervals.

This project has the potential to induce a ground-breaking change in constitutive modelling—from user-defined model selection to automated model discovery—which would forever change how we simulate materials and structures.

Section b. Methodology

IV. SCIENTIFIC APPROACH

Throughout this research, I will pursue a holistic scientific approach that seamlessly integrates theory, experiment, and computation to automatically discover the best model, parameters, and experiment that explain a wide variety of soft matter systems. My research methodology requires a deep knowledge in constitutive modelling, soft matter physics, machine learning, and artificial intelligence, and is designed around three work packages, as illustrated in Figure 8.

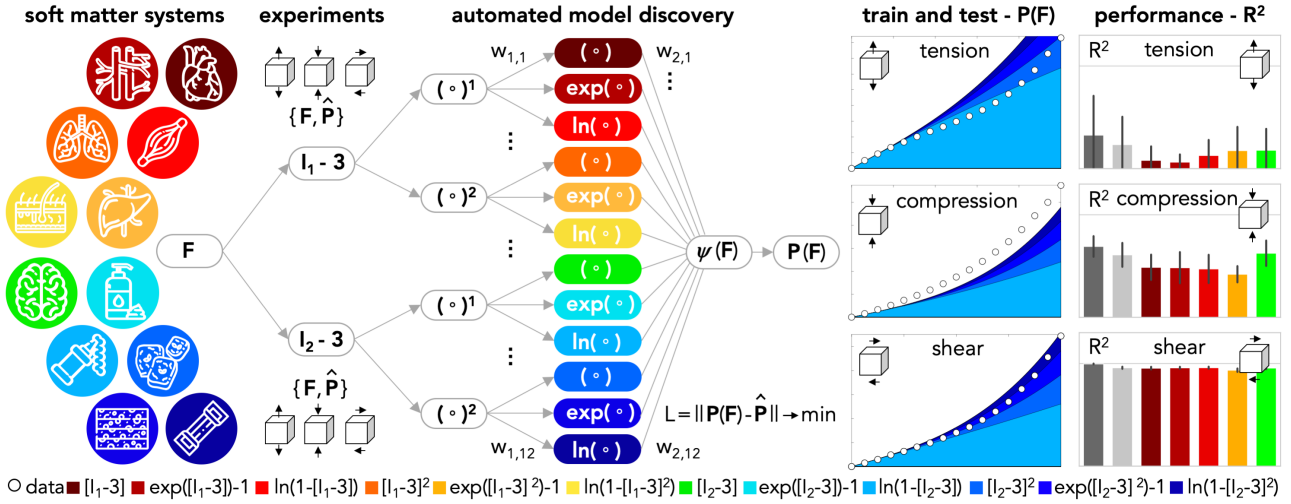

Figure 8. Automated model discovery. Discovering the best model, parameters, and experiment to explain a wide variety of soft matter systems including the heart, arteries, muscle, lung, liver, skin, brain, hydrogels, silicone, artificial meat, foams, and rubber. I will establish a new family of neural networks; train, test and validate them on tension, compression, and shear data; quantify their performance on new multiaxial experiments; and embed them into a Bayesian analysis to quantify uncertainty.

WP 1. Establish a new family of constitutive neural networks that reproducibly discover the model, parameters, and experiment that best explain a wide variety of soft matter systems.

Introduction. Soft materials play an integral role in many aspects of modern life including biomedicine, energy storage, and consumer goods, and their accurate modeling is critical to understand their unique properties and functions. A recent trend in soft material modeling is to entirely abandon existing constitutive models and fully replace them by neural networks. However, classical neural networks perform poorly on small data, they ignore the fundamental laws of physics, and their parameters have no physical interpretation. The *objective* of this work package is to build, train, and test *my own* family of constitutive neural networks that a priori satisfy the fundamental laws of physics through selective input, output, architecture, and activation functions. ***My hypothesis is that my new constitutive neural networks seamlessly integrate our prior domain knowledge in soft matter physics and autonomously discover the model and parameters that best explain a wide variety of soft materials***. My *approach* is to reverse-engineer a neural network-like structure from the functional building blocks of popular constitutive models and hardwire physical constraints into the network design. Importantly, our network weights naturally translate into meaningful parameters with physical units and a real physical interpretation. The *rationale* for using machine learning to automate model selection is that this allows us to rapidly screen millions of possible models, confirm existing models, and autonomously discover new combinations of terms, which are out of reach for conventional manual decision making today. My *expectation* is that our custom-designed networks will induce a paradigm shift in constitutive modeling, from user-defined to fully automated, which will make modeling accessible to a more inclusive and diverse community and accelerate scientific discovery and innovation.

Justification and Feasibility. Our new family of constitutive neural networks combines decades of research on the mechanics of materials and structures with state-of-the-art technologies in machine learning. By incorporating our prior domain knowledge, instead of using existing neural networks as a black box[118], we simplify the network architecture, make it more reliable and efficient, and ensure that it complies with basic physical principles[6,9,94,129]. Mathematically speaking, model selection is a highly nonlinear nonconvex optimization problem that we could, in principle, solve with classical optimization schemes or system identification[14,15,16,35,54,78,137,138]. Instead, we formulate model selection as a custom-designed network to exploit the power of adaptive gradient-descent based optimizers developed for deep learning[67]. We have prototyped this idea for rubber[74], skin[76,126], muscle[136]and human brain[75], using invariant-based[74] and principal-stretch-based[123] networks, and envision that combining both into a single architecture to analyze other soft materials will be conceptually feasible and straightforward.

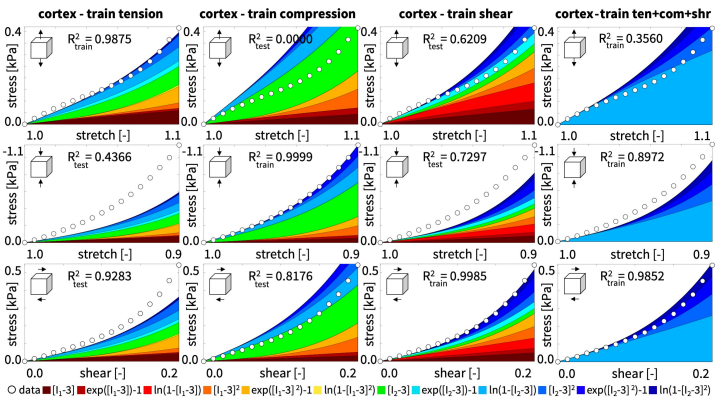

Figure 9. Automated model discovery for human brain tissue. Stress as a function of stretch and shear strain; dots illustrate the tension, compression, and shear data; color code highlights the discovered model; individual training with R_{train}^2 on the diagonal, testing with R_{test}^2 on off-diagonal, and combined training with R_{train}^2 in the right column.

Research Design. In WP1, I will reverse-engineer a new family of constitutive neural networks for soft matter systems from the functional building blocks of popular constitutive models. My research design for WP1 uses a four-step approach that tightly integrates building a family of constitutive neural networks, training the networks on single loading modes, testing the networks on previously unseen loading modes, and discovering the best models and parameters for selected soft matter systems.

WP 1.1. Build a family of constitutive neural networks for soft matter systems. First, we will build a new family of constitutive neural networks that combine our invariant-based[75] and principal-stretch-based[123,133] neural networks into a selectively connected feed-forward constitutive neural network architecture with two invariants, I_1 and I_2, and two principal stretches, λ_1 and λ_2, as input. From these

kinematic descriptors, I will calculate four input terms that are zero in the reference configuration, [I_1 - 3] and [I_2 - 3] as well as [$\lambda_1^2 + \lambda_2^2 + \lambda_3^2$ - 3] and [$\lambda_1^{-2} + \lambda_2^{-2} + \lambda_3^{-2}$ – 3]. The network will have two hidden layers, and seven activation functions for all four inputs, $(o)^1$, $(o)^2$, $(o)^n$, $\exp(o)^1$-1, $\exp(o)^2$-1, $\ln(1-(o)^1)$, $\ln(1-(o)^2)$, scaled by twelve weights, see Figure 10. This will result in 4 x 7 = 28 individual terms and 4 x 12 = 48 network parameters, $\boldsymbol{w} = w_{ij}$. Importantly, by constraining our network input, output, activation functions, and architecture, in contrast to classical off-the-shelf neural networks, our custom designed network will a priori satisfy thermodynamic consistency, material objectivity, material symmetry, and polyconvexity.

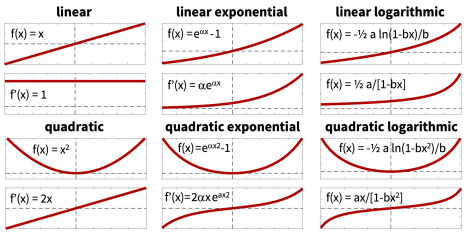

Figure 10. Custom-designed activation functions reverse-engineered from the main building blocks of popular constitutive models are central to our approach[75].

WP 1.2. Train the networks on soft matter data from a single loading mode. Second, we will train our networks on soft matter data including classical benchmark data for rubber[132], data from our collaborators for skin[125], arteries[87], and the heart[51], and our own data for human brain[18]. We will train the network on soft matter data from the single loading modes of tension, compression, and shear, and for comparison, for all three loading modes combined. We will minimize the loss function, $L(\boldsymbol{w}; \boldsymbol{F}) = \|\boldsymbol{P}(\boldsymbol{F}) - \boldsymbol{P}\|^2 / n_{train} \rightarrow \min$, the error between model $\boldsymbol{P}(\boldsymbol{F})$ and data $\{\boldsymbol{F}, \boldsymbol{P}\}$ divided by the number of training points n_{train}, using the Adam optimizer, a robust adaptive algorithm for gradient-based first-order optimization[74]. We expect the loss function to converge robustly within 10,000 epochs[75]. For batch sizes of 32, we expect each training run to take 3-5 minutes on a standard desktop computer. Our experience shows that, during this process, the majority of our 48 network weights will train to zero. The small subset of non-zero weights defines the best model. Our new 28-term network will discover this model from 2^{28} = 268,435,456 possible combinations of terms, from more than 250 million possible models!

WP 1.3. Test the networks on previously unseen data from different modes. Third, will test our networks on previously unseen data using the unused modes of tension, compression, and shear that we have not previously used for training in WP1.2. We will characterize the performance of the discovered model and parameters by comparing the computationally modeled and experimentally measured stress-stretch relations in terms of the goodness of fit, R_{train}^2 and R_{test}^2, that we will calculate separately for training and testing[75]. For completeness, we will also calculate and report the normalized mean squared errors for training and testing[136]. From our experience, we expect the networks to train well on individual tension, compression, and shear tests, with R_{train}^2 values consistently close to one as Figure 9 suggests. We expect the network to test well for materials that are tension-compression symmetric, but less well for tension-compression asymmetric materials like the human brain[21]: Networks trained on tension data alone could potentially perform poorly when tested with compression data, in extreme cases with R_{test}^2 values close to zero[75]. For comparison, we will also train the network on all three loading modes combined, and expect a less perfect fit than for training with individual data sets, with R_{train}^2 values on the order of 0.9[126].

WP 1.4. Discover models and parameters for a wide variety of soft materials. Fourth, we will explore the generalizability and performance of our discovery platform by discovering models and parameters for other published soft matter data from silicone, foams, hydrogels, liver, cartilage, and arteries[87]. Importantly, our network weights naturally translate into meaningful parameters with physical units and a real physical interpretation, for example stiffnesses E, shear moduli μ, or Lamé constants L and G. To validate our discovery platform, for each material, we will compare our discovered parameters against the material parameters reported in the literature. Unfortunately, there is only a very limited number of well-documented studies that perform all three modes of testing, tension, compression, and shear on one and the same specimen[21,86]. This has inspired WP2, where we will perform our own systematic series of experiments for model training, testing, and validation on previously unseen data.

Deliverables and Potential Limitations. WP1 will generate several exciting deliverables including: (i) a general concept to hardwire physical knowledge into a neural network design; (ii) a new family of constitutive neural networks for incompressible, hyperelastic materials; (iii) a set of mechanistically interpretable network weights that are intrinsically related to traditional invariant- and principal-stretch-based parameters; and (iv) a new open-source discovery platform to autonomously discover model,

parameters, and experiments for soft matter systems that I will make publicly available on GitHub @LivingMatterLab. While our preliminary results suggest that we can robustly and repeatedly discovery a small subset of non-zero network weights that define model selection and parameterization[74,75,76,126], there is a chance that the discovery process identifies a large set of terms or becomes non-unique. To mitigate this limitation and reduce the potential risk of overfitting, I will apply L1 and L2 regularization, $L(\boldsymbol{w}; \boldsymbol{F}) = ||\boldsymbol{P}(\boldsymbol{F}) - \boldsymbol{P}||^2 / n_{train} + \alpha_1 ||\mathbf{w}||_1 + \alpha_2 ||\mathbf{w}||_2^2 \rightarrow$ min, by supplementing the loss function with the weighted L1 norm $||\mathbf{w}||_1$ or the weighted L2 norm $||\mathbf{w}||_2^2$. We have shown that increasing the parameters α_1 and α_2 reduces the number of non-zero weights and with it the number of activated terms[75,123,136]. I am confident that appropriate regularization will stabilize our model discovery. Another limitation that we have successfully addressed in the past is that we may need to constrain the network parameters to always remain non-negative to ensure polyconvexity[6,9,75,124]. Importantly, in WP1, we will only discover point values for these parameters. Embedding our approach into a Bayesian analysis[66,72] in WP3 will further stabilize the method by discovering parameter distributions with means and credible intervals.

WP 2. Train, test, and validate our discovered models on previously unseen data for the heart, arteries, muscle, lung, liver, skin, brain, hydrogels, silicone, artificial meat, foams, and rubber.

Introduction. Benchmarking material models is critical to quantify their performance and accuracy against other models and evaluate their potential to solve real-world problems. To date, most constitutive neural networks are benchmarked against artificial synthetic data, but their true performance on noisy and incomplete real world-data remains insufficiently understood. The *objective* of this work package is to perform a series of tension, compression, and shear experiments on a variety of soft materials to train, test, and validate our model. ***My hypothesis is that our discovered models will outperform popular existing models and generalize robustly to previously unseen data in the spirit of continuous learning.*** To test this hypothesis, I will use a combined experimental-computational *approach* and perform a series of tension, compression, and shear experiments on 5x5x5mm^3 cubic samples of both natural and man-made soft materials to generate new, previously unseen data for network training, testing, and validation. I will quantify the performance of model discovery for the heart, arteries, muscle, lung, liver, skin, brain, hydrogels, silicone, artificial meat, foams, and rubber using the coefficients of determination during training and testing, R_{train}^2 and R_{test}^2, and normalized root mean squared errors, and compare our discovered models against a variety of popular existing models. The *rationale* for systematic benchmarking with traditional models is that this will confirm successful existing models, identify shortcomings in others, and build trust in our newly discovered models. It is my *expectation* that our open source benchmark library, with dozens of data sets, models, and parameters, will become a standard go to reference that will increase collaboration, reusability, transparency, and learning opportunities that will benefit both individual soft matter modelers and the mechanics community at large.

Justification and Feasibility. Our preliminary studies in Figure 7 solidly suggest that the loss function of our constitutive neural network converges consistently within less than 5,000 epochs[75]. For single mode training with individual tension, compression, or shear data, our model discovery is generally non-unique[74] and all weights are activated, as we conclude from the rainbow-type color spectrum in the first three columns of Figures 7 and 9. Yet, for multi-mode training with all three data sets combined, in the right column, the network repeatably discovers the same four-term model[75], $\psi(I_2) = \frac{1}{2}\mu_2[I_2 - 3]^2 + \frac{1}{2}a_2/b_2[\exp(b_2[I_2-3]^2) - 1] - \frac{1}{2}\alpha_1/\beta_1 \ln(1-(\beta_1[I_2 - 3])) - \frac{1}{2}\alpha_2/\beta_2 \ln(1-(\beta_2[I_2 - 3]^2))$. Strikingly, this best-fit model only features the second invariant I_2. This is in stark contrast with the widely used first invariant

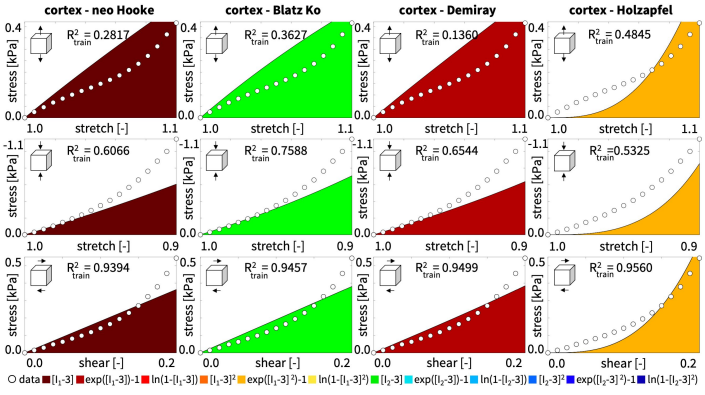

Figure 11. Special cases of neo Hooke, Blatz Ko, Demiray, and Holzapfel models. Stress as a function of stretch and shear strain; dots illustrate tension, compression, and shear data; color code highlights terms of the model in Figure 6 with goodness of fit R_{train}^2.

based neo Hooke model[131], $\psi = \frac{1}{2}\ \mu\ [\ I_1 - 3\ ]$, Demiray model[23], $\psi = \frac{1}{2}\ a/b\ [\exp(b\ [\ I_1 - 3\ ]) - 1]$, and Gent model[40], $\psi = -\frac{1}{2}\ \alpha/\beta\ \ln(1-(\beta\ [\ I_1 - 3\ ]))$, and justifies using a more holistic machine learning approach to identify model terms that have been overlooked in the past, but provide a better fit. We will build on our preliminary studies for brain tissue[18], and now perform multiaxial tension, compression, and shear tests on other soft matter systems. Our experience shows that, while data from different loading modes are necessary for unique and repeatable model discovery, approximately twelve data points per curve are generally sufficient for successful training and testing[123,136].

Research Design. In WP2, I will perform a series of multiaxial benchmark experiments to generate an open source library of for network training, testing, and validation. My research design for WP2 uses an integrative four-step approach that systematically performs new multiaxial experiments to collect previously unseen data, expands our network architecture to discover the best model and parameters, learns the parameters of popular traditional models, and compares our newly discovered models against a variety of traditional models.

WP 2.1. Perform a series of multiaxial tests on natural and man-made soft matter systems. First, we will probe the generalizability of our approach by performing a comprehensive series of benchmark experiments to generate new, previously unseen data for network training, testing, and validation. Together with the senior staff scientist of this project, I will visit Professor Gerhard Holzapfel's group at TU Graz to train myself in multiaxial soft tissue testing[18-20,49,52,87]. I will then purchase the same triaxial testing device (Zwick/Roell, Ulm, Germany) to perform *new* tension, compression, and shear experiments on up to $5 \times 5 \times 5\,mm^3$ large cubic specimens of both natural and man-made soft materials following our previous protocols[18]. I will expand our existing library for rubber[74], skin[76], muscle[136], and brain[75] on GitHub @LivingMatterLab and successively add our new experimental data. First, we will test man-made materials with tunable material properties including rubber[59,99,103,132], foams, silicone, hydrogels, and artificial meat. Next, we will test biological samples. Initially, we will test animal samples of the heart[51,109], arteries[49], muscle[104-106,136], lung[30,31], liver, skin[68,69,76,108,], and brain[18,27,32,44] from a nearby slaughterhouse to optimize our testing protocols. Then, we will gradually move to human samples, which are routinely tested both at the Institute for Biomechanics at TU Graz and at the Chair of Applied Mechanics at FAU Erlangen, approved by the Ethics Committees of the TU Graz and FAU Erlangen under approval numbers 25-420ex12/13 and 405_18B, respectively. This will generate a comprehensive benchmark library with data from tension, compression, and shear stretch-stress pairs $\{\lambda, P\}_i$ or $\{\gamma, P\}_i$ for dozens of soft matter experiments. We have previously shown i = 1, …, 12 data pairs are generally sufficient for successful training and testing[75], although we will also make the raw data available.

WP 2.2. Discover the best model and parameters from all possible models. Second, we will use our model discovery platform from WP 1 to discover the best model, parameters, and experiments across all data in our open source library. This will result in deliverables similar to Figure 9, with individual training displayed on the diagonal, individual testing displayed on the off-diagonal, and combined training for all three modes displayed in the right column[75,123,136]. We expect that a limitation of our neural network from WP1 is that not all of our materials will be incompressible and isotropic. Specifically, we expect that at least the heart, arteries, muscle, skin, and artificial muscle will be anisotropic[36,62,125,143]. To address the limitation of incompressibility and isotropy of our networks from WP 1, we will add the third, fourth, and fifth invariants[29,46,82,119], I_3, I_4, I_5, or rather their representations in the undeformed reference configuration, $[I_3 - 1]$, $[I_4 - 1]$, $[I_5 - 1]$, to our network architecture, and discover the best model, parameters, and experiments across all data in our open source library. While we have previously shown that the weights of the fifth invariant

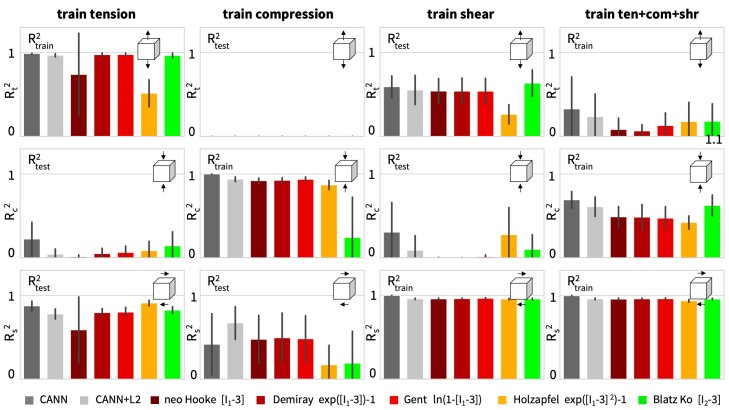

Figure 12. Goodness of fit R_{train}^2 and R_{test}^2 for our discovered model compared to traditional models. Our method in gray outperforms the classical neo Hooke, Demiray, Gent, Holzapfel, and Blatz Ko models in dark red, red, light red, orange, and green, both in training and testing[75].

I_5 tend to train to zero for skin[76], we will still keep it for completeness for all twelve materials. We expect to discover models with two, three, or four leading terms, and have shown that we can modulate the number of vanishing weights through L1 or L2 regularization[75,123,136] to systematically control the number of relevant terms in our models.

WP 2.3. Learn the best parameters for popular traditional constitutive models. Third, we will use our network architecture to learn the best parameters of popular constitutive models, similar to a traditional parameter identification[57,63,107,117]. Specifically, we will constrain all but a few selected network weights to zero, and use our network to learn the best parameters of widely used classical models including the neo Hooke model[131] with $\psi = ½\,\mu\,[I_1\text{-}3]$, the Demiray model[23] with $\psi = ½\,a/b\,[\exp(b[I_1\text{-}3])\text{-}1]$, the Gent model[40] with $\psi = -½\,\alpha/\beta\,\ln(1\text{-}(\beta[I_1\text{-}3]))$, the Holzapfel model[49] with $\psi = ½\,a/b\,[\exp(b[I_4\text{-}3])^2\text{-}1]$, and the Blatz Ko[12] model with $\psi = ½\,\mu\,[I_2\text{-}3]$. We will compare our learned parameters to the parameters reported in the literature, including shear moduli, stiffnesses, and exponential coefficients. This comparison will confirm both our experimental method and our parameter discovery.

WP 2.4. Compare the performance of newly discovered models to traditional models. Fourth, we will systematically compare our newly discovered models from WP 2.2 to the traditional models from WP 2.3. Specifically, during both training and testing, we will calculate the R_{train}^2 and R_{test}^2 values and the normalized root mean squared errors to quantify the goodness of fit of all models similar to Figure 13. The goodness of fit R^2 for human brain data in Figure 12 suggests that our newly discovered model with and without L2 regularization highlighted through the grey bars consistently outperforms the traditional neo Hooke[131], Demiray[23], Gent[40], Holzapfel[49], and Blatz Ko[12] models highlighted through the dark red, red, light red, orange, and green bars. The rationale for systematic benchmarking with traditional models is that this will confirm successful existing models, identify shortcomings in others, and build trust in our newly discovered models. We will also benchmark our constitutive neural networks against more recent data-driven approaches[28,45,61,96], including symbolic[1,2,116] or sparse[14,26,34,35,] regression, system identification[137,138], and classical parameter identification[18,63,83,86]. We will share all data, models, and parameters of this work packages, in our open source library on GitHub @LivingMatterLab for other potential users to reproduce our results, train their own networks, benchmark their results, or simply use our models and parameters for their own soft material simulations.

Deliverables and Potential Limitations. The deliverables of WP2 are: (i) a comprehensive experimental data sets of soft matter systems including the heart, arteries, muscle, lung, liver, skin, brain, hydrogels, silicone, artificial meat, foams, and rubber, (ii) a suite of newly discovered models and parameters for natural and man-made soft materials; (iii) a quantitative performance evaluation of our newly discovered models compared to existing traditional models; and (iv) new mechanistic insight into the fundamental building blocks of constitutive models for soft matter systems. I expect that our open source benchmark library, with dozens of new data sets, models, and parameters, will become a standard go to reference that will increase collaboration, reusability, transparency, and learning opportunities that will benefit both individual soft matter modelers and the mechanics community at large. We recognize that our proposed approach is initially limited to isotropic hyperelastic materials. We have recently prototyped a feed forward neural network for transversely isotropic materials by including the fourth and fifth invariants, I_4 and I_5, and successfully discovered models and parameters for skin[76,126], see Figure 15. We have also prototyped a recurrent neural network for viscoelastic materials by treating the viscous overstress as history variable, and discovered the model, elastic parameters, and viscoelastic long-term modulus and relaxation times for muscle[136], see Figure 13. If

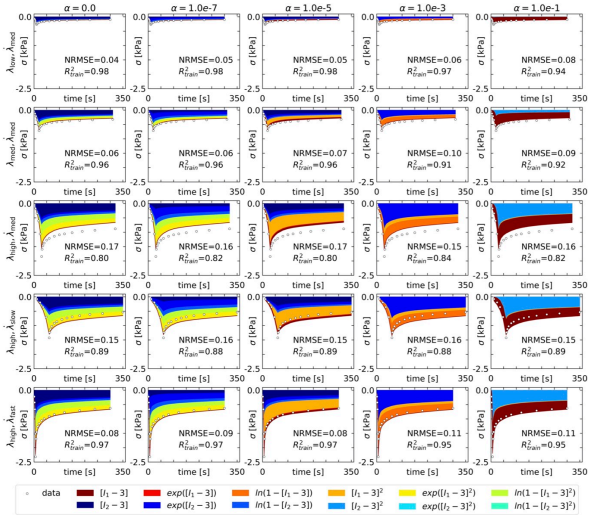

Figure 13. Automated model discovery for passive skeletal muscle. Stress as a function of stretch and stretch rate; dots illustrate stress relaxation data; color code highlights the discovered viscoelastic model; increasing the regularization from α = 0.0, left, to α = 0.1, right, selectively reduces the number of discovered terms.

necessary, it will be straightforward to expand our network to compressible[46], transversely isotropic[76], or orthotropic[51], viscoelastic[99,100,136] materials, or, potentially even include other types of inelasticity such as damage[24,135], plasticity, or even poroelasticity. A more involved limitation is the lack of sufficient train, test, and validation data. We conclude from our experience in Figures 7 and 9 that model discovery can become non-unique when discovering parameter point values in single mode training. This is why it will be critical to purchase our own test system and have 24/7 access to a triaxial test facility to always be able to go back and collect more data if needed. In general, we do expect that embedding our approach into a Bayesian analysis in WP3 will stabilize our method by discovering parameter distributions with means and credible intervals[54,66,72], instead of single parameter point values.

WP 3. Quantify the uncertainty of our models, parameters, and experiments by embedding our networks into a Bayesian analysis to discover parameter distributions and credible intervals.

Neural networks have been successfully used to fit stress-stretch curves to data; yet, to date, no unified concept exists to interpret the data, model, and parameters in view of uncertainty quantification. The *objective* of this work package is to establish a family of Bayesian constitutive neural networks to discover models, parameters distributions, and credible intervals for uncertainty quantification. ***My hypothesis is that by embedding our networks into a Bayesian framework, our deterministic model, and parameter point estimates from WP1 and WP2 will seamlessly translate into probabilistic models and parameter distributions for uncertainty quantification.*** I will test this hypothesis by adopting an iterative experimental-computational *approach* and embed our trained neural networks in a Bayesian analysis; discover probabilistic models, parameter distributions, and experiments that best explain prior data; perform new experiments; update our prior beliefs; and iteratively repeat this cycle to narrow our credible intervals. My *rationale* is that the weights of our Bayesian constitutive neural networks represent well-defined physical parameters with means and credible intervals that will progressively narrow as more new data become available. This progressive updating is a form of continuous learning in which the model continuously improves the understanding of its parameters based on new information. Once validated across a wide range of soft matter data, it is my *expectation* that our probabilistic model discovery platform will not only accurately reproduce and predict the behavior of soft material systems in complex real-life situations, but also provide a more complete picture of our model uncertainties and support a more robust and reliable decision making.

Justification and Feasibility. We will build on our physics informed Bayesian neural networks for real-world nonlinear dynamical systems[72], where we have successfully used Bayes' theorem[10], $p(\vartheta|\boldsymbol{P}) = p(\boldsymbol{P}|\vartheta)/p(\vartheta) \cdot p(\boldsymbol{P})$, to estimate the posterior probability distribution of the network parameters $\vartheta = \{w_{ij}\}$ such that the statistics of the neural network agree with the experimental data $\boldsymbol{P}$. Here $p(\boldsymbol{P}|\vartheta)$ is the likelihood, the conditional probability of the data $\boldsymbol{P}$ for given fixed network parameters ϑ; $p(\vartheta)$ is the prior, the probability distribution of the network parameters ϑ; $p(\boldsymbol{P})$ is the marginal likelihood; and $p(\vartheta|\boldsymbol{P})$ is the posterior, the conditional probability of the network parameters ϑ for the given data $\boldsymbol{P}$[66]. We have previously embedded a reaction-diffusion model for Alzheimer's disease in a Bayesian analysis and shown that tau misfolding and brain shrinkage are larger in the diseased group than in healthy controls[114,115], see Figure 14. We have also successfully applied Bayesian neural networks in the spirit of continuous learning to simulate the outbreak dynamics of Covid-19 by adding new disease data in real time[66,70,90] and to simulate soft biomimetic actuators inspired by the elephant trunk[55,56]. Our results suggest that our physics informed Bayesian neural networks outperform traditional Bayesian neural networks and have better

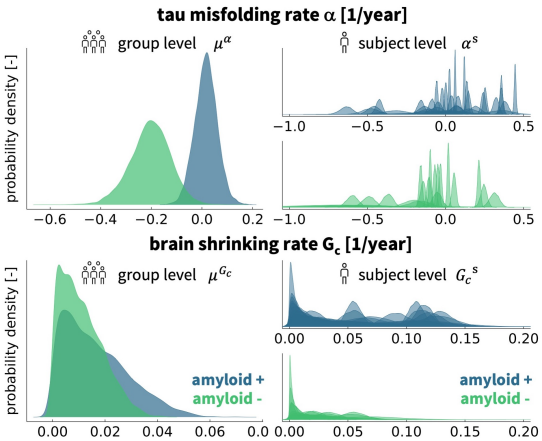

Figure 14. Our Bayesian analysis of tau misfolding and brain shrinking in a reaction-diffusion model for Alzheimer's disease shows that misfolding and shrinking are larger in the diseased group, shown in blue, than in the healthy group, shown in green[115].

predictive potential and narrower credible intervals[72]. From this experience, we believe that translating this approach to our constitutive neural networks from WP1 and WP2 is generally feasible and relatively straightforward. To disseminate this new technology to a broad user audience, we have started a partnership with Abaqus FEA/Simulia to explore the feasibility of integrating all this knowledge into a single universal user material subroutine for simulations in Abaqus and other finite element platforms.

Research Design. In WP3, I will quantify the uncertainty of our models, parameters, and experiments to build confidence in my approach and support more robust and reliable simulations. My research design for WP3 uses an integrative four step approach that embeds our constitutive neural networks into a Bayesian analysis; tests and trains the Bayesian network on our soft matter data from WP2; iteratively discovers better models, parameters distributions, and credible intervals; and, ultimately, embeds all this knowledge into a single universal material subroutine for finite element analyses.

WP 3.1. Build a family of Bayesian constitutive neural networks for soft matter systems. First, I will embed our constitutive neural networks from WP1 into a Bayesian framework. My objective is to use Bayes' theorem[10], $p(\vartheta|\boldsymbol{P}) = p(\boldsymbol{P}|\vartheta)/p(\vartheta) \cdot p(\boldsymbol{P})$, to estimate the posterior parameter distributions, $p(\vartheta|\boldsymbol{P})$, of a set of network parameters $\vartheta = \{w_{ij}\}$, such that the statistics of the network output $\boldsymbol{P} = \partial\psi(\vartheta)/\partial\boldsymbol{F}$ agree with our experimental data $\boldsymbol{P}$. Here $p(\boldsymbol{P}|\vartheta)$ is the likelihood, the product of the individual point-wise likelihoods for each deformation level of our data set, for which we select a normal distribution $\mathcal{N}(\mu,\sigma)$, where the mean μ is the output of our model $P_{ij} = \partial\psi(\vartheta)/\partial F_{ij}$ for given network parameters ϑ, and σ is the likelihood width, i.e., the standard deviation, for example $\sigma = 0.05$[66]. For the prior probability distributions $p(\vartheta)$, we will select weakly informed priors[72], informed by our prior knowledge from WP1 and WP2, with normal distributions $\mathcal{N}(\mu,\sigma)$ with a zero-mean $\mu = 0$ for all network parameters, $\vartheta = \{w_{ij}\}$.

WP 3.2. Train and test the Bayesian networks on soft matter data. Second, we will train and test our new Bayesian constitutive neural networks on our newly collected data from WP2.1. Importantly, instead of using the means of the data to discover point values of parameters as we have done in WP2.2, we will now use each individual data set to discover parameter distributions with means and credible intervals[72]. Specifically, we will infer the posterior parameter distributions $p(\vartheta|\boldsymbol{P})$ using Bayes' theorem[10] and employ Hamilton Monte Carlo sampling using Tensorflow-Probability. Using our previous protocols, we will use the first 3000 samples to tune the sampler and the subsequent 3000 samples to estimate the conditional probability of the network parameters ϑ for our given experimental data $\boldsymbol{P}$. In contrast to WP2.2., where we learn point values for the network weights ϑ, our Bayesian neural network now learns probability distributions for the network weights, from which we can extract means, credible intervals, and uncertainty to make probabilistic predictions[115]. Importantly, unlike standard Bayesian neural networks for which the network weights are random variables without any real physical interpretation, our custom-designed Bayesian networks learn distributions of physics-based parameters such as stiffnesses E, shear moduli μ, or Lamé constants L and G, with means and credible intervals that teach us something about the underlying physics[72].

WP 3.3. Iteratively discover better models, parameter distributions, and credible intervals. Third, we will iteratively discover better models for the heart, arteries, muscle, lung, liver, skin, brain, hydrogels, silicone, artificial meat, foams, and rubber by gradually performing more experiments to narrow our credible intervals. Specifically, our Bayesian analysis in WP3.2 will infer the best probabilistic model, posterior parameter distributions, $p(\vartheta|\boldsymbol{P}) = p(\boldsymbol{P}|\vartheta) / p(\vartheta) \cdot p(\boldsymbol{P})$, and experiment to explain our previous data. This discovery step will inform the design of new experiments with the highest possible degree of information. We will perform these discovered experiments, use our new experimental data to update our prior probability distributions, $p(\vartheta)$, and start a new learning cycle. Importantly, our

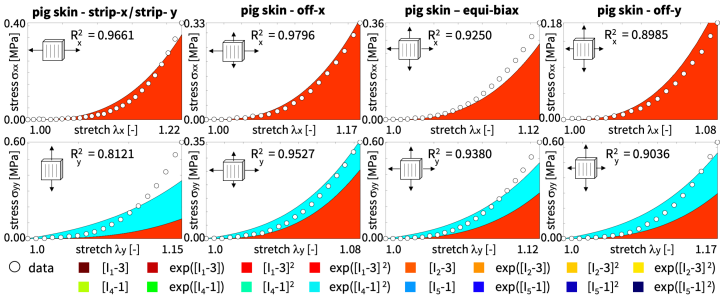

Figure 15. Automated model discovery for skin. Stress as a function of stretch; dots illustrate biaxial extension data; color code highlights the discovered model; R_x^2 and R_y^2 values suggest that the off-x test with the largest R^2 values is the best experiment[76].

Bayesian approach represents a form of continuous learning[70,90] that progressively integrates new knowledge in the form of newly recorded stretch-stress pairs, $\{\lambda, P\}_i$. It naturally enables uncertainty quantification[54,66] from the inferred posterior parameter distributions, $p(\vartheta|\boldsymbol{P})$. As the network is exposed to more and more data, it will progressively improve its performance. We will quantify performance improvement by calculating and comparing the coefficients of determination R^2 and the width of the inferred credible intervals. I will successively add our new experimental data, probabilistic models, and parameter distributions to our open source library on GitHub @LivingMatterLab.

WP 3.4. Integrate all knowledge into a single universal material subroutine. Finally, to make our new technology available to a broad user audience, I will integrate our gained knowledge into a single universal material subroutine. To mitigate the potential high risk associated with this objective, I have initiated a partnership with Abaqus FEA/Simulia. Together, we are exploring the feasibility of creating a user interface that seamlessly takes our network output as input and selectively activates a few terms that define the best model and parameters to perform realistic finite element simulations of soft matter systems. We will build on our current prototype based on the network in Figure 6, and integrate the third, fourth, and fifth invariants, I_3, I_4, I_5, to add compressibility and transverse isotropy[76]. Next, we will add features of mixed invariants, I_1 and I_3, or I_1 and I_4, to incorporate pressure-sensitive effects like the Poynting effect[83]. This will be more cumbersome, especially in implicit codes like Abaqus standard, since these terms will introduce more involved derivatives in the stress and tangent expressions. First, we will validate our implementation against our homogeneous tension, compression, and shear benchmarks from WP1 and WP2 in our open source library similar to Figure 16. Then, we will perform heterogeneous finite element simulations of our samples in tension, compression, and shear to explore to which extent the assumption of homogeneity under- or over-estimates the soft matter stiffness as indicated in Figure 17. Finally, we will perform finite element simulations of complex real-life systems to demonstrate the generalizability of our discovered models, similar to the examples in Figure 18. We will simulate both man-made and natural soft matter systems[8,38,128]. Yet, we envision the highest gain for simulations of realistic biological systems, for which in vivo stresses play a critical role in clinical decision making[44,111,122], disease management[39,91,109,112,145], or personalized treatment design [92,98,110], where stress measurements in the living body are out of reach with current diagnostic technologies today.

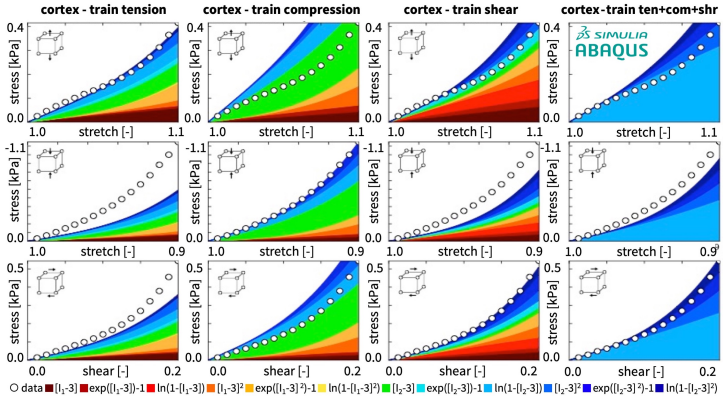

Figure 16. Validation of universal material subroutine. Stress as a function of stretch and shear strain; dots illustrate the tension, compression, and shear data; color code highlights the discovered model according to Figure 6, but now simulated with our new universal user materials subroutine. The finite element simulation accurately reproduces the initial stress response in Figure 9.

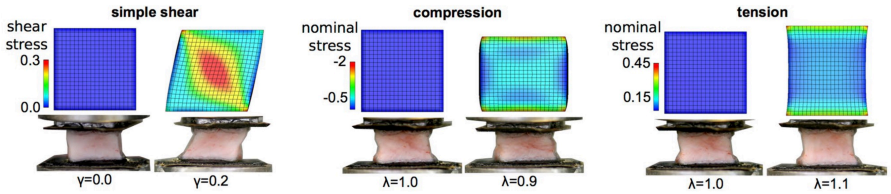

Figure 17. Effects of inhomogeneous deformation. We will perform finite element simulations to explore the heterogeneous nature of the deformation and stress profiles to investigate whether and to which extent the assumption of homogeneity under- or over-estimates the soft matter stiffness in shear, compression, and tension[21].

Deliverables and Potential Limitations. The deliverables of WP3 are: (i) a novel iterative technology to seamlessly integrate experiment and computation using Bayesian constitutive neural networks; (ii) a suite of newly discovered probabilistic models and parameter distributions for a wide variety of natural and man-made soft materials; (iii) a fully trained, tested, and validated continuously learning discovery platform for soft matter systems; and (iv) a universal material subroutine for finite element simulations that will replace dozens of individual material-specific subroutines. While our preliminary results suggest that Bayesian regularization stabilizes network training—even on sparse and noisy data—the lack of sufficiently rich data remains a general limitation of neural networks. Importantly, we can always return to collect more data, for example for combined loading modes, treat our previously inferred distributions

as priors, and calculate new posterior distributions[66,70,90]. If anisotropic effects turn out to be dominant, we will include additional invariants, similar to Figure 15, which will also allow us to discover microstructural features such as fiber or sheet orientations, fiber dispersion, or volume fractions[49-52]. If coupling effects turn out to be relevant, we will revisit our sparsely connected network architecture and introduce edges between individual invariants, for example between I_1 and I_3 to capture the Poynting effect[83] or shear thinning, or between I_1 and I_4 to capture fiber dispersion[51]. If viscous effects turn out to be important, we will replace our feed forward architecture by a recurrent neural network[136], which will allow us to model dynamic behavior and discover characteristic time constants of the material[78,128,134]. While we expect to address most of the limitations of our man-made materials, one shortcoming that is inherent to natural materials will remain: the ex vivo nature of our model and parameter discovery. We will address this potential limitation by applying our universal material subroutine to perform forward finite element simulations and quantify the difference between our discovered ex vivo material properties and the in vivo properties from our previous inverse finite element simulations[38,91,109] or from our magnetic resonance elastography based stiffness measurements[139,141,142].

V. EXPECTED IMPACT

This project integrates cutting-edge developments in constitutive modeling, soft matter physics, deep learning, and artificial intelligence. This unique synergy will advance knowledge and provide innovative new technologies including: (i) a new design paradigm to reverse-engineer constitutive neural networks from the functional building blocks of popular constitutive models; (ii) a robust and efficient strategy to translate network weights into physically interpretable engineering parameters; (iii) the first family of constitutive neural networks that simultaneously discover the best models, parameters, and experiments—out of more than a million possible models—to characterize soft matter systems; (iv) a comprehensive open source library with dozens of data sets for natural and man-made soft materials including the heart, arteries, muscle, lung, liver, skin, brain, hydrogels, silicone, artificial meat, foams, and rubber; and (v) an open source discovery platform with our constitutive neural networks, models, and parameters to promote engineering education and advance scientific knowledge. This research is truly transformative in that it will enable a fully automated model, parameter, and experiment discovery, entirely without human interaction. ***This project has the potential to revolutionize constitutive modeling, from user-defined model selection to automated model discovery, which would forever change how we simulate materials and structures.***

This project will inspire the new multidisciplinary course *Automated Model Discovery* at the interface of engineering science and artificial intelligence. It will leverage large experimental undergraduate and graduate courses in which students perform multiaxial tests on soft biological tissues to crowdsource a large user group and probe model discovery on previously unseen data. I am in close discussion with Springer Nature with the objective to publish the content of the course in the textbook *Automated Model Discovery*. Table 1 summarizes the timeline of this project with work packages W1, W2, W3 and major milestones and deliverables throughout years 1 to 5. ***My main deliverable is a fully documented open source scientific discovery platform that includes our neural networks, experimental data, benchmarks, models, and parameters, freely accessible on GitHub for a wide range of users, regardless of their institutional or financial resources.***

To broaden participation across the entire European Union and beyond, I will actively recruit users with diverse backgrounds at short courses and summer schools, and produce short educational videos. I expect that automated model discovery will lower the barrier of entry into science, technology, engineering, and mathematics, stimulate a more inclusive and diverse scientific and technological community, and, ultimately, enable a more comprehensive understanding of soft matter systems.

To foster technology transfer, I have partnered with Dassault Systemès Simulia to integrate our automated model discovery directly into their Abaqus finite element workflow and translate this knowledge into engineering practice. This technology has the potential to generate several exciting by-products of groundbreaking nature. For example, it would enable real-life simulations that critically depend on accurate constitutive models to calculate stress profiles across the human body in vivo. These

high-resolution stress profiles are out of reach with current diagnostic technologies today; yet, they are highly significant in clinical decision making. for example, during brain development[25,47,64], neurosurgery[140], traumatic brain injury[44], and neuro-degenerative diseases[33,65,112,113] as illustrated in Figure 18. As a founding member of the Abaqus Living Heart Project, I will leverage my successful collaboration with Dassault Systemès Simulia[8,39,91,92,98, 109-111,122] and embed automated model discovery into Abaqus simulations. Integrating our discovery platform into a finite element analysis will not only allow us to accurately reproduce and predict the behavior of soft material systems in complex real-life situations, but also provide a more complete picture of model uncertainties, and support a more robust and reliable decision making, especially with applications in the benefit of human health.

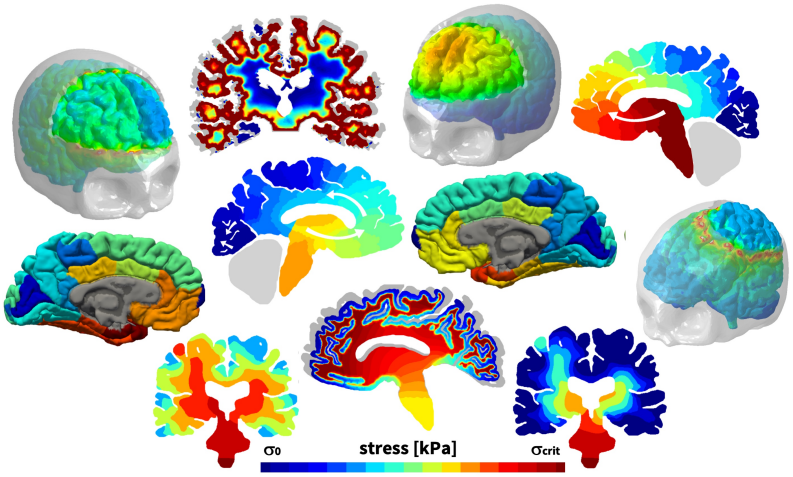

Figure 16. My group routinely performs clinically significant real-life simulations that critically depend on accurate constitutive models to calculate stress profiles in vivo, for example, in the human brain during brain development[25,47,64], neurosurgery[140], traumatic brain injury[44], and neurodegenerative diseases[33,65,112,113]. This project will enable more realistic simulations and make computational modeling broadly accessible to a more inclusive and diverse community.

This project has broad scientific, social, and economic impact, in that it will democratize constitutive modeling, stimulate discovery in soft matter systems, provide enabling machine-learning inspired tools to characterize, create, and functionalize soft matter, and train the next generation of civil, mechanical, and manufacturing innovators to adopt and promote these new technologies.

Table 1. Timeline of the proposed project with work packages W1, W2, W3 and major milestones in years 1 through 5.

		Y1	Y2	Y3	Y4	Y5
WP 1	***Establish a new family of constitutive neural networks that reproducibly discover the model, parameters, and experiment that best explain a wide variety of soft matter systems.***					
WP 1.1	Build a family of constitutive neural networks for soft matter systems.	■	■			
WP 1.2	Train the networks on soft matter data from a single loading mode.	■	■	■		
WP 1.3	Test the networks on soft matter data from different modes.		■	■		
WP 1.4	Discover models and parameters for a wide variety of soft materials.		■	■		
WP 2	***Train, test, and validate our discovered models on previously unseen data for the heart, arteries, muscle, lung, liver, skin, brain, hydrogels, silicone, artificial meat, foams, and rubber.***					
WP 2.1	Perform a series of multiaxial tests on natural and man-made soft matter systems.	■	■	■		
WP 2.2	Discover the best model and parameters from all possible models.		■	■		
WP 2.3	Learn the best parameters for popular traditional constitutive models.		■	■		
WP 2.4	Compare the performance of newly discovered models to traditional models.			■	■	
WP 3	***Quantify the uncertainty of our models, parameters, and experiments by embedding our networks into a Bayesian analysis to discover parameter distributions and credible intervals.***					
WP 3.1	Build a family of Bayesian constitutive neural networks for soft matter systems.		■	■		
WP 3.2	Train and test the Bayesian networks on soft matter data sets.			■	■	
WP 3.3	Iteratively discover better models, parameter distributions, and credible intervals.			■	■	■
WP 3.4	Integrate all knowledge into a single universal material subroutine.				■	■

Literature [Kuhl's students and postdocs underlined]

1. Abdusalamov R, Pandit R, Milow B, Itskov M, Rege A (2021) Machine learning-based structure-property predictions in silica aerogels. Soft Matter 17: 7350-7358.
2. Abdusalamov R, Hillgärtner M, Itskov M (2023) Automatic generation of interpretable hyperelastic material models by symbolic regression. International Journal for Numerical Methods in Engineering 124: 2093-2104.
3. Aldakheel, Satari R, Wriggers P (2021) Feed-forward neural networks for failure mechanics problems. Applied Science 11: 6483.
4. Aldakheel F, Elsayed ES, Zohdi TI, Wriggers P (2023) Efficient multiscale modeling of heterogeneous materials using deep neural networks. Computational Mechanics, in press.
5. Alber M, Buganza Tepole A, Cannon W, De S, Dura-Bernal S, Garikipati K, Karniadakis GE, Lytton WW, Perdikaris P, Petzold L, **Kuhl E** (2019) Integrating machine learning and multiscale modeling: Perspectives, challenges, and opportunities in the biological, biomedical, and behavioral sciences. npj Digital Medicine 2:115.
6. Antman SS (2005) Nonlinear Problems of Elasticity. Second edition. Springer-Verlag New York.
7. As'ad F, Avery P, Farhat C (2022) A mechanics-informed artificial neural network approach in data-driven constitutive modeling. International Journal for Numerical Methods in Engineering 123: 2738 - 2759.
8. Baillargeon B, Rebelo N, Fox DD, Taylor RL, **Kuhl E** (2014) The Living Heart Project: A robust and integrative simulator for human heart function. European Journal of Mechanics A/Solids 48: 38-47.
9. Ball JM (1977) Convexity conditions and existence theorems in nonlinear elasticity. Archive for Rational Mechanics and Analysis 63: 337-403.
10. Bayes T, Price R (1763) An Essay towards Solving a Problem in the Doctrine of Chances. By the Late Rev. Mr. Bayes, F.R.S. communicated by Mr. Price, in a Letter to John Canton, Philosophical Transactions of the Royal Society of London. 53:370–418.
11. Bhouri MA, Sahli Costabal F, Wang H, Linka K, Peirlinck M, **Kuhl E**, Perdikaris P (2021) COVID-19 dynamics across the US: A deep learning study of human mobility and social behavior. Computer Methods in Applied Mechanics and Engineering 382: 113891.
12. Blatz PJ, Ko WL (1962) Application of finite elastic theory to the deformation of rubbery materials. Transactions of the Society of Rheology 6:223-251.
13. Bongard J, Lipson H (2007) Automated reverse engineering of nonlinear dynamical systems. Proceedings of the National Academy of Sciences 104: 9943-9948.
14. Brunton SL, Proctor JL, Kutz N (2016) Discovering governing equations from data by sparse identification of nonlinear dynamical systems. Proceedings of the National Academy of Sciences 113: 3932-3937.
15. Brunton SL, Kutz N (2019) Methods for data-driven multiscale model discovery for materials. Journal of Physics: Materials 2: 044002.
16. Brunton SL, Kutz N (2022) Data-Driven Science and Engineering. 2nd Edition. Cambridge University Press, Cambrdige.
17. Budday S, Nay R, de Rooij R, Steinmann P, Wyrobek T, Ovaert TC, **Kuhl E** (2015) Mechanical properties of gray and white matter brain tissue by indentation. Journal of the Mechanical Behavior of Biomedical Materials 46: 318-330.
18. Budday S, Sommer G, Birkl C, Langkammer C, Jaybaeck J, Kohnert, Bauer M, Paulsen F, Steinmann P, **Kuhl E**, Holzapfel GA (2017) Mechanical characterization of human brain tissue. Acta Biomaterialia 48: 319-340.
19. Budday S, Sommer G, Hayback J, Steinmann P, Holzapfel GA, **Kuhl E** (2017) Rheological characterization of human brain tissue. Acta Biomaterialia 60:315-329.
20. Budday S, Sommer G, Holzapfel GA, Steinmann P, **Kuhl** E (2017) Viscoelastic parameter identification of human brain tissue. Journal of the Mechanical Behavior of Biomedical Materials 74: 463-476.
21. Budday S, Ovaert TC, Holzapfel GA, Steinmann P, **Kuhl E** (2020) Fifty shades of brain: A review on the material testing and modeling of brain tissue. Archives of Computational Methods in Engineering 27:1187–1230.
22. Defino A, Stergiopulos N, Moore JE, Meister JJ (1997) Residual strain effects of the stress field in a thick wall finite element model of the human carotid bifurcation. Journal of Biomechanics 30: 777-786.
23. Demiray H (1972) A note on the elasticity of soft biological tissues. Journal of Biomechanics 5: 309-311.
24. de Rooij R, **Kuhl E** (2018) Microtubule polymerization and cross-link dynamics explain axonal stiffness and damage. Biophysical Journal 114: 201-212.
25. de Rooij R, **Kuhl E** (2018) A physical multifield model predicts the development of volume and structure in the human brain. Journal of the Mechanics and Physics of Solids. 112: 563-576.

26. de Silva BM, Higdon DM, Brunton SL, Kutz N (2020) Discovery of physics from data: Universal laws and discrepancies. Frontiers of Artificial Intelligence 3:25.
27. Destrade M, Gilchrist MD, Murphy JG, Rashid B, Saccomandi G (2015) Extreme softness of brain matter in simple shear. International Journal of Non-Linear Mechanics 75: 54–58.
28. Eggersmann R, Kirchendoerfer T, Reese S, Stainier L, Ortiz M (2019) Model-free data-driven inelasticity. Computer Methods in Applied Mechanics and Engineering 350: 81-99.
29. Ehret AE, Itskov M (2007) A polyconvex hyperelastic model for fiber-reinforced materials in application to soft tissues. Journal of Material Science 42: 8853–8863.
30. Eskandari M, Pfaller MR, **Kuhl E** (2013) On the role of mechanics in chronic lung disease. Materials 6: 5639-5658.
31. Eskandari M, Javili A, **Kuhl E** (2016) Elastosis during airway wall remodeling explains multiple coexisting instability patterns. Journal of Theoretical Biology 403: 209-218.
32. Faber J, Hinrichsen J, Greiner A, Reiter N, Budday S (2022) Tissue-scale biomechanical testing of brain tissue for the calibration of nonlinear material models. Current Protocols 2: e381.
33. Fornari S, Schafer A, Jucker M, Goriely A, **Kuhl E** (2019) Prion-like spreading of Alzheimer's disease within the brain's connectome. Journal of the Royal Society Interface 16: 20190356.
34. Flaschel M, Kumar S, De Lorenzis L (2021) Unsupervised discovery of interpretable hyperelastic constitutive laws. Computer Methods in Applied Mechanics and Engineering 381: 113852.
35. Flaschel M, Kumar S, De Lorenzis L (2023) Automated discovery of generalized standard materials models with EUCLID. Computer Methods in Applied Mechanics and Engineering 405: 115867.
36. Fuhg JN, Bouklas N (2022) On physics-informed data-driven isotropic and anisotropic constitutive models through probabilistic machine learning and space-filling sampling. Computer Methods in Applied Mechanics and Engineering 394: 114915.
37. Fuhg JN, Bouklas N, Jones RE (2022) Learning hyperelastic anisotropy from data via a tensor basis neural network. Journal of the Mechanics and Physics of Solids 168: 105022.
38. Genet M, Rausch MK, Lee LC, Choy S, Zhao X, Kassab GS, Kozerke S, Guccione JM, **Kuhl E** (2015) Heterogeneous growth-induced prestrain in the heart. Journal of Biomechanics 48: 2080-2089.
39. Genet M, Lee LC, Baillargeon B, Guccione JM, **Kuhl E** (2016) Modeling pathologies of systolic and diastolic heart failure. Annals of Biomedical Engineering 44: 112-127.
40. Gent A (1996) A new constitutive relation for rubber. Rubber Chemistry and Technology 69: 59-61.
41. Ghaboussi J, Garrett JH, Wu X (1991) Knowledge-based modeling of material behavior with neural networks. Journal of Engineering Mechanics 117: 132-153.
42. Ghaderi A, Morovati V, Dargazany R (2020) A physics-informed assembly for feed-forward neural network engines to predict inelasticity in cross-linked polymers. Polymers 12: 2628.
43. Goriely A, Budday S, **Kuhl E** (2015) Neuromechanics: from neurons to brain. Advances in Applied Mechanics 48: 79-139.
44. Goriely A, Geers MGD, Holzapfel GA, Jayamohan J, Jerusalem A, Sivaloganathan S, Squier W, van Dommelen JAW, Waters S, **Kuhl E** (2015) Mechanics of the brain: Perspectives, challenges, and opportunities. Biomechanics and Modeling in Mechanobiology 14: 931-965.
45. Harandi A, Moeineddin A, Kaliske M, Reese S, Rezaei S (2023) Mixed formulation of physics-informed neural networks for thermos-mechanically coupled systems and heterogeneous domains. arXiv, doi:10.48550/arXiv.2303.04954.
46. Hartmann S, Neff P (2003) Polyconvexity of generalized polynomial-type hyperelastic strain energy functions for near-incompressibility. International Journal of Solids and Structures 40: 2767-2791.
47. Holland MA, Budday S, Goriely A, **Kuhl E** (2018) Symmetry breaking in wrinkling patterns: Gyri are universally thicker than sulci. Physical Review Letters 121: 228002.
48. Holzapfel GA, Simo JC (1996) Entropy elasticity of isotropic rubber-like solids at finite strains. Computer Methods in Applied Mechanics and Engineering 132: 17-44.
49. Holzapfel GA, Gasser TC, Ogden RW (2000) A new constitutive framework for arterial wall mechanics and comparative study of material models. Journal of Elasticity 61:1-48.
50. Holzapfel GA (2000) Nonlinear Solid Mechanics: A Continuum Approach to Engineering. John Wiley & Sons, Chichester.
51. Holzapfel, Ogden (2009) Constitutive modeling of passive myocardium: a structurally based framework for material characterization. Philosophical Transactions of the Royal Society A 367: 3445-3476.

52. Holzapfel GA, Linka K, Sherifova S, Cyron C (2021) Predictive constitutive modelling of arteries by deep learning. Journal of the Royal Society Interface 18:20210411.
53. Hopfield JJ (1982) Neural networks and physical systems with emergent collective computational abilities. Proceedings of the National Academy of Science 79:2554-2558.
54. Joshi A, Thakolkaran P, Zheng Y, Escande M, Flaschel M, De Lorenzis L, Kumar S (2022) Bayesian-EUKLID: Discovering hyperelastic mateirals laws with uncertainties. Computer Methods in Applied Mechanics and Engineering 398: 115225.
55. Kaczmarski B, Moulton DE, Goriely A, **Kuhl E** (2023) Bayesian design optimization of biomimetic soft actuators. Computer Methods in Applied Mechanics and Engineering 408: 115939.
56. Kaczmarski B, Goriely A, **Kuhl E**, Moulton DE (2023) A simulation tool for physics-informed control of biomimetic soft robotic arms. IEEE Robotic Automation Letters 8: 936-943.
57. Kakaletsis S, Lejeune E, Rausch MK (2023) Can machine learning accelerate soft material parameter identification from complex mechanical test data? Biomechanics and Modeling in Mechanobiology 22: 57-70.
58. Kalina KA, Linden L, Brummund J, Metsch P, Kastner M (2022) Automated constitutive modeling of isotropic hyperelasticity based on artificial neural networks. Computational Mechanics 69: 213-232.
59. Kaliske M, Rothert H (1997) On the finite element implementation of rubber-like materials at finite strains. Engineering Computations 14: 216-232.
60. Karniadakis GE, Kevrekidis IG, Lu L, Perdikaris P, Wang S, Yang L (2021) Physics-informed machine learning. Nature Reviews Physics 3:422-440.
61. Kirchendoerfer T, Ortiz M (2016) Data-driven computational mechanics. Computer Mathods in Applied Mechanics and Engineering 304: 81-101.
62. Klein DK, Fernandez M, Martin RJ, Neff P, Weeger O (2022) Polyconvex anisotropic hyperelasticity with neural networks. Journal of the Mechanics and Physics of Solics 159: 105703.
63. Kleuter B, Menzel A, Steinmann P (2007) Generalized parameter identification for finite viscoelasticity. Computer Methods in Applied Mechanics and Engineering 196: 3315-3334.
64. **Kuhl E** (2016) Biophysics: Unfolding the brain. Nature Physics 12: 533-534.
65. **Kuhl E** (2019) Connectomics of neurodegeneration. Nature Neuroscience 22: 1200–1202.
66. **Kuhl E** (2021) Computational Epidemiology. Data-driven modeling of COVID-19. Springer Nature.
67. LeCun Y, Bengio Y, Hinton G (2015) Deep learning. Nature 521: 436-444.
68. Limbert G, **Kuhl E** (2018) On skin microrelief and the emergence of expression microwrinkles. Soft Matter 14: 1292-1300.
69. Limbert G (2019) Skin Biophysics: From Experimental Characterisation to Advanced Modelling. Springer Nature Switzerland.
70. Linka K, Peirlinck M, Sahli Costabal F, **Kuhl E** (2020) Outbreak dynamics of COVID-19 in Europe and the effect of travel restrictions. Computer Methods in Biomechanics and Biomedical Engineering 23:710-717.
71. Linka K, Hillgartner M, Abdolazizi KP, Aydin RC, Itskov M, Cyron CJ (2021) Constitutive artificial neural networks: A fast and general approach to predictive data-driven constitutive modeling by deep learning. Journal of Computational Physics 429: 110010.
72. Linka K, Schafer A, Meng X, Zou Z, Karniadakis GE, **Kuhl E** (2022) Bayesian Physics-Informed Neural Networks for real-world nonlinear dynamical systems. Computer Methods in Applied Mechanics and Engineering 402: 115346.
73. Linka K, Cavinato C, Humphrey JD, Cyron CJ (2022) Predicting and understanding arterial elasticity from key microstructural features by bidirectional deep learning by deep learning. Acta Biomaterialia 147: 63-72.
74. Linka K, **Kuhl E** (2023) A new family of Constitutive Artificial Neural Networks towards automated model discovery. Computer Methods in Applied Mechanics and Engineering 403: 115731.
75. Linka K, St Pierre SR, **Kuhl E** (2023) Automated model discovery for human brain using Constitutive Artificial Neural Networks. Acta Biomaterialia 160: 134-151.
76. Linka K, Buganza Tepole A, Holzapfel GA, **Kuhl E** (2023) Automated model discovery for skin: Discovering the best model, data, and experiment. Computer Methods in Applied Mechanics and Engineering 410: 116007.
77. Mahnken R (2022) Strain mode-dependent weighting functions in hyperelasticity accounting for verification, validation, and stability of material parameters. Archive of Applied Mechanics 92: 713-754.
78. Marino E, Flaschel M, Kumar S, De Lorenzis L (2023) Automated identification of linear viscoelastic constitutive laws with EUKLID. Mechanics of Materials 181: 104643.

79. Masi F, Stefanou I, Vannucci P, Maffi-Berthier V (2021) Thermodynamics-based artificial neural networks for constitutive modeling. Journal of the Mechanics and Physics of Solids 147: 04277.
80. Masi F, Stefanou I (2022) Multiscale modeling of inelastic materials with Thermodynamics-based Artificial Neural Networks (TANN). Computer Methods in Applied Mechanics and Engineering 398: 115190.
81. McCulloch WS, Pitts W (1943) A logical calculus of the ideas immanent in nervous activity. Bulletin of Mathematical Biophysics 5: 115–133.
82. Menzel A, Steinmann P (2003) A view on anisotropic finite hyperelasticity. European Journal of Mechanics A/Solids 22:71-87.
83. Mihai LA, Chin L, Janmey PA, Goriely A (2015) A comparison of hyperelastic constitutive models applicable to brain and fat tissues. Journal of the Royal Society Interface 12: 20150486.
84. Mihai LA, Budday S, Holzapfel GA, **Kuhl E**, Goriely A (2017) A family of hyperelastic models for human brain tissue. Journal of the Mechanics and Physics of Solids 106: 60-79.
85. Mooney M (1940) A theory of large elastic deformations. Journal of Applied Physics 11: 582-590.
86. Moran R, Smith JH, Garcia JJ (2014) Fitted hyperelastic parameters for human brain tissue from reported tension, compression, and shear tests. Journal of Biomechanics 47: 3762-3766.
87. Niestrawska JA, Viertler C, Regitnig P, Cohnert TU, Sommer G, Holzapfel GA (2016) Microstructure and mechanics of healthy and aneurysmatic abdominal aortas: experimental analysis and modelling. Journal of the Royal Society Interface 13: 20160620.
88. Noll W (1958) A mathematical theory of the mechanical behavior of continuous media. Archive of Rational Mechanics Analysis 2: 197-226.
89. Ogden RW (1972) Large deformation isotropic elasticity - on the correlation of theory and experiment for incompressible rubberlike solids. Proceedings of the Royal Society London Series A 326: 565-584.
90. Peirlinck M, Linka K, Sahli Costabal F, **Kuhl E** (2020) Outbreak dynamics of COVID-19 in China and the United States. Biomechanics and Modelingin Mechanobiology 19: 2179-2193.
91. Peirlinck M, Sahli Costabal F, Sack KL, Choy JS, Kassab GS, Guccione JM, De Beule M, Segers P, **Kuhl E** (2019) Using machine learning to characterize heart failure across the scales. Biomechanics Modeling and Mechanobiology 18: 1987-2001.
92. Peirlinck M, Sahli Costabal F, Yao J, Guccione JM, Tripathy S, Wang Y, Ozturk D, Segars P, Morrison TM, Levine S, **Kuhl E** (2021) Precision medicine in human heart modeling. Perspectives, challenges and opportunities. Biomechanics Modeling and Mechanobiology 20: 803-831.
93. Peng GCY, Alber M, Buganza Tepole A}}, Cannon W, De S, Dura-Bernal S, Garikipati K, Karniadakis G, Lytton WW, Perdikaris P, Petzold L, **Kuhl E** (2021) Multiscale modeling meets machine learning: What can we learn? Archives of Computer Methods in Engineering 28: 1017-1037.
94. Planck M (1897) Vorlesungen über Thermodynamik. Verag von Veit & Comp. Leipzig.
95. Ploch CC, Mansi CSSA, Jayamohan J, **Kuhl E** (2016) Using 3D printing to create personalized brain models for neurosurgical training and preoperative planning. World Neurosurgery 90: 668-674.
96. Prume E, Reese S, Ortiz M (2023) Model-free data-driven inference in computational mechanics. Computer Methods in Applied Mechanics and Engineering 403: 115704.
97. Raissi M, Perdikaris P, Karniadakis GE (2019) Physics-informed neural networks: a deep learning framework for solving forward and inverse problems involving nonlinear partial differential equations. Journal of Computational Physics 378:686–707.
98. Rausch MK, Zollner AM, Genet M, Baillargeon B, Bothe W, **Kuhl E** (2017) A virtual sizing tool for mitral valve annuloplasty. International Journal for Numerical Methods in Biomedical Engineering 33: e02788.
99. Reese S, Govindjee S (1997) Theoretical and numerical aspects in the thermo-viscoelastic material behavior of rubber-like polymers. Mechanics of Time-Dependent Materials 1: 357-396.
100. Reese S, Govindee S (1998) A theory of finite viscoelasticity and numerical aspects. International Journal of Solids and Structures 35: 3455-3482.
101. Rezaei S, Harandi A, Moeineddin A, Xu BX, Reese S (2022) A mixed formulation for physics-informed neural networks as a potential solver for engineering problems in heterogeneous domains: Comparison with finite element method. Computer Methods in Applied Mechanics and Engineering 401: 115616.
102. Rivlin RS (1948) Large elastic deformations of isotropic materials. IV. Further developments of the general theory. Philosophical Transactions of the Royal Society of London Series A 241: 379–397.
103. Rivlin RS, Sauders DW (1951) Large elastic deformations of isotropic materials. VII. Experiments on the deformation of rubber. Philosophical Transactions of the Royal Society of London Series A 243: 251-288.

104. Röhrle O, Pullan AJ (2007) Three-dimensional finite element modelling of muscle forces during mastication. Journal of Biomechanics 40: 3363-3372.
105. Röhrle O (2010) Simulating the electro-mechanical behavior of skeletal muscles. Computing in Science & Engineering 12: 48-58.
106. Röhrle O, Davidson JB, Pullan AJ (2012) A physiologically based, multi-scale model of skeletal muscle structure and function. Frontiers in Physiology 3: 358.
107. Rose L, Menzel A (2020) Optimisation based material parameter identification using full field displacement and temperature measurements. Mechanics of Materials 145: 103292.
108. Sachs D, Wahlsten A, Kozerke S, Restivo G, Mazza E (2021) A biphasic multiplayer computational model of human skin. Biomechanics and Modeling in Mechanobiology 20: 969-982.
109. Sahli Costabal F, Choy JS, Sack KL, Guccione JM, Kassab G, **Kuhl E** (2019) Multiscale characterization of heart failure. Acta Biomaterialia 86: 66-76.
110. Sahli Costabal F, Matsuno K, Yao J, Perdikaris P, **Kuhl E** (2019) Machine learning in drug development: Characterizing the effect of 30 drugs on the QT interval using Gaussian process regression, sensitivity analysis, and uncertainty quantification. Computer Methods in Applied Mechanics and Engineering 348: 313-333.
111. Sahli Costabal F, Seo K, Ashley E, **Kuhl E** (2020) Classifying drugs by their arrhythmogenic risk using machine learning. Biophysical Journal 118: 1-12.
112. Schafer A, Weickenmeier J, **Kuhl E** (2019) The interplay of biochemical and biomechanical degeneration in Alzheimer's disease. Computer Methods in Applied Mechanics and Engineering 352: 369-388.
113. Schafer A, Chaggar P, Thompson TB, Goriely A, **Kuhl E** (2021) Predicting brain atrophy from tau pathology: a summary of clinical findings and their translation into personalized models. Brain Multiphysics. 2: 100039.
114. Schafer A, Peirlinck M, Linka K, **Kuhl E** (2021) Bayesian physics-based modeling of tau propagation in Alzheimer's disease. Frontiers in Physiology. 12: 702975.
115. Schafer A, Chaggar P, Goriely A, **Kuhl E** (2022) Correlating tau pathology to brain atrophy using a physics-based Bayesian model. Engineering with Computers 38: 3867-3877.
116. Schmidt M, Lipson H (2009) Distilling free-form natural laws from experimental data. Science 324: 81-85.
117. Schulte R, Karca C, Ostwald R, Menzel A (2022) Machine learning-assisted parameter identification for constitutive models based on concatenated loading path sequences. European Journal of Mechanics A/Solids 98: 104854.
118. Shen Y, Chandrashekhara K, Breig WF, Oliver LR (2004) Neural Network based constitutive model for rubber material. Rubber Chemistry and Technology 77: 257-277.
119. Spencer AJM (1971) Theory of Invariants. In: Eringen AC, Ed., Continuum Physics Vol. 1: 239-353, Academic Press, New York.
120. Sprave L, Menzel A (2020) A large strain gradient-enhanced ductile damage model: finite element formulation, experiment and parameter identification. Acta Mechanica 231: 5159-5192.
121. Steinmann P, Hossain M, Possart G (2012) Hyperelastic models for rubber-like materials: consistent tangent operators and suitability for Treloar's data. Archive of Applied Mechanics 82:1183-1217.
122. St Pierre SR, Peirlinck M, **Kuhl E** (2022) Sex matters: A comprehensive comparison of female and male hearts. Frontiers in Physiology 13: 831179.
123. St Pierre SR, Linka K, **Kuhl E** (2023) Principal-stretch-based constitutive neural networks autonomously discover a subclass of Ogden models for human brain tissue. Brain Multiphysics 4: 100066.
124. Tac V, Sahli Costabal F, Buganza Tepole A (2022) Data-driven tissue mechanics with polyconvex neural ordinary differential equations. Computer Methods in Applied Mechanics and Engineering 398: 115248.
125. Tac V, Sree VD, Rausch MK, Buganza Tepole A (2022) Data-driven modeling of the mechanical behavior of anisotropic soft biological tissue. Engineering with Computers 38: 4167-4182.
126. Tac V, Linka K, Sahli Costabal F, **Kuhl E**, Buganza Tepole A (2023) Benchmarks for physics-informed data-driven hyperelasticity. Computational Mechanics, in press, arXiv doi:10.1101/2022.11.08.515656.
127. Thakolkaran P, Joshi A, Zheng Y, Flaschel M, De Lorenzis L, Kumar S (2022) NN-EUKLID: Deep-learning hyperelasticity without stress data. Journal of the Mechanics and Physics of Solids 169: 105076.
128. Tikenogullari OZ, Sahli Costabal F, Yao J, Marsden A, **Kuhl E** (2022) How viscous is the beating heart? Insights from a computational study. Computational Mechanics 70: 565-579.
129. Truesdell C, Noll W (1965) Non-linear field theories of mechanics. In: Flügge S, Ed., Encyclopedia of Physics, Vol. III/3, Spinger, Berlin.
130. Truesdell C (1969) Rational Thermodynamics, Lecture 5. McGraw-Hill, New York.

131. Treloar LRG (1944) Stress-strain data for vulcanised rubber under various types of deformation. Transactions of the Faraday Society 40: 59-70.
132. Treloar LRG (1948) Stresses and birefringence in rubber subjected to general homogeneous strain. Proceedings of the Physical Society 60: 135-144.
133. Valanis KC, Landel RF (1967) The strain-energy function of hyperelastic materials in terms of extension ratios. Journal of Applied Physics 38: 2997-3002.
134. Wang LM, **Kuhl E** (2020) Viscoelasticity of the axon limits stretch-mediated growth. Computational Mechanics 65: 587-595.
135. Wang LM, **Kuhl E** (2023) Mechanics of axon growth and damage: A systematic review of computational models. Seminars in Cell and Developmental Biology 140: 13-21.
136. Wang LM, Linka K, **Kuhl E** (2023) Automated model discovery for muscle using constitutive recurrent neural networks. bioRxiv, doi:10.1101/2023.05.09.540027.
137. Wang Z, Huan X, Garikipati K (2019) Variational system identification of partial differential equations governing the physics of pattern formation: Inference under varying fidelity and noise. Computer Methods in Applied Mechanics and Engineering 356:4 4-74.
138. Wang Z, Estrada JB, Arruda EM, Garikipati K (2021) Inference of deformation mechanisms and constitutive response of soft material surrogates of biological tissue by full-field characterization and data-driven variational system identification. Journal of the Mechanics and Physics of Solids. 153: 104474.
139. Weickenmeier J, de Rooij R, Budday S, Steinmann P, Ovaert TC, **Kuhl E** (2016) Brain stiffness increases with myelin content. Acta Biomaterialia 42: 265-272.
140. Weickenmeier J, Butler CAM, Young PG, Goriely A, **Kuhl E** (2017) The mechanics of decompressive craniectomy: Personalized simulations. Computer Methods in Applied Mechanics and Engineering 314: 180-195.
141. Weickenmeier J, Kurt M, Ozkaya E, Wintermark M, Butts Pauly K, **Kuhl E** (2018) Magnetic resonance elastography of the brain: A comparison between pigs and humans. Journal of the Mechanical Behavior of Biomedical Materials 77:702-710.
142. Weickenmeier J, Kurt M, Ozkaya E, de Rooij R, Ovaert TC, Ehman RL, Butts Pauly K, **Kuhl E** (2018) Brain stiffens post mortem. Journal of the Mechanical Behavior of Biomedical Materials 84: 88-98.
143. Weiss JA, Maker BN, Govindjee S (1996) Finite element implementation of incompressible, transversely isotropic hyperelasticity. Computer Methods in Applied Mechanics and Engineering. 135: 107-128.
144. Zhang X, Garikipati K (2020) Machine learning material physics: Multi-resolution neural networks learn the free energy and nonlinear elastic response of evolving microstructures. Computer Methods in Applied Mechanics and Engineering 372: 113362.
145. Zollner AM, Pok JM, McWalter EJ, Gold GE, **Kuhl E** (2015) On high heels and short muscles: A multiscale model for sarcomere loss in the gastrocnemius muscle. Journal of Theoretical Biology 365: 301–310.
146. Zopf C, Kaliske M (2017) Numerical characterisation of uncured elastomers by a neural network based approach. Computers and Structures 182: 504-525.